Macromolecules

Article

pubs.acs.org/Macromolecules

Theoretical Mechanistic Studies on the *trans*-1,4-Specific Polymerization of Isoprene Catalyzed by a Cationic La–Al Binuclear Complex

Xiaohui Kang,[†] Yi Luo,*[,†] Guangli Zhou,[†] Xingbao Wang,[†] Xuerong Yu,[†] Zhaomin Hou,[†,‡] and Jingping Qu[†]

[†]State Key Laboratory of Fine Chemicals, School of Pharmaceutical Science and Technology, Dalian University of Technology, Dalian 116024, China

[‡]RIKEN Center for Sustainable Resource Science, Organometallic Chemistry Laboratory, RIKEN, 2-1 Hirosawa, Wako, Saitama 351-0198, Japan

Supporting Information

ABSTRACT: This paper reports a DFT study on *trans*-1,4-specific polymerization of isoprene catalyzed by the cationic heterobimetallic half-sandwich complex $[(C_5Me_5)La(AlMe_4)]^+$. The possible structures of the active species, viz., $[(C_5Me_5)La(\mu_2\text{-}Me)_3AlMe]^+$ (**A**), $[(C_5Me_5)La(\mu_2\text{-}Me)_2AlMe_2]^+$ (**B**), and $[(C_5Me_5)La(Me)(\mu_2\text{-}Me)AlMe_2]^+$ (**C**), have been investigated. On the basis of the chain initiation and the structure transformations among these three species, **C** has been proposed to be the true active species smoothly producing *trans*-1,4-polyisoprene observed experimentally. Both La/Al bimetal-cooperating monomer insertion and La-center-based insertion pathways have been calculated, and the latter is found to be more favorable, where the $AlMe_3$ moiety serves as a ligand coordinating to the La center via a methyl group. In contrast to this, in the Y analogous system, the $AlMe_3$ ligand is proposed to leave away from the Y center during the chain propagation and the *cis*-1,4-selectivity is preferred, showing a consistence with experimental results. Such a situation could be ascribed to the smaller ionic radius of Y and thermodynamically favorable dissociation of $AlMe_3$ from Y center in comparison with the La system. These results suggest that such an alkylaluminum compound plays a crucial role in the regulation of selectivity in the polymerization system investigated.

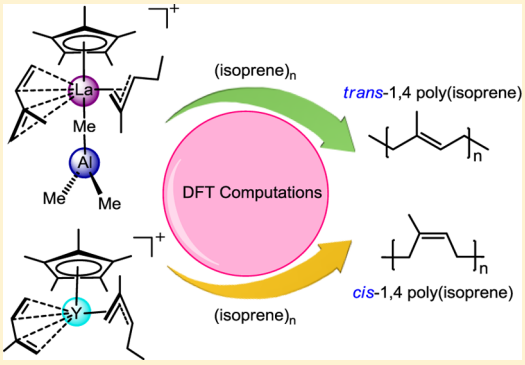

INTRODUCTION

Polyisoprenes with versatile microstructures show different chemical, physical, and mechanical properties. *cis*-1,4-Polyisoprene (>99% *cis* content), featuring low melting point, high solubility, and high elasticity, is a key component of natural rubber for tires and adhesives,[1] whereas its isomer *trans*-1,4-polyisoprene called Gutta-percha is thermoplastic crystalline polymer with high hardness and high tensile strength, mainly used as the medical materials and a key component of tire sides and tread rubbers.[2] Thus far, the precise control on the microstructure of the isoprene polymers with specific properties has remained a very attractive and everlasting topic. In this context, polymers of isoprene have been widely synthesized by numerous heterogeneous Ziegler–Natta catalysts based on group 4 and late transition metals such as Ti, Co, Ni, and Cr.[3] However, the activity, selectivity, and more-gel formation of 1,3-dienes polymerization remain to be improved. By contrast, the well-defined Ziegler–Natta rare-earth metal precursors[2b] with Nd metal as a pioneer showed the most promising potentials for conjugated dienes polymerization and copolymerization and afforded polymers with outstanding properties. Beyond that, it was interesting to find that the strong dependence of the catalytic performance on the metal center and the alkylaluminum compounds (e.g., MAO: methylaluminoxane; MMAO: modified methylaluminoxane; TMA: trimethylaluminum; TEA: triethylaluminum; TIBA: triisobutylaluminum, etc.). For instance, the neodymium isopropoxide $Nd(O^iPr)_3$[4a] together with cocatalyst MAO showed high efficiency in isoprene polymerization at low [Al]/[Nd] ratios, and the generated polyisoprene has high *cis*-1,4-content (90%), high molecular weight ($M_n = 10^5$), and narrow molecular weight distribution ($M_w/M_n = 1.9–2.8$). However, the combination of $Nd(O^iPr)_3$ with MMAO gave relatively lower yield and lower molecular weight of the resulting polymer. In the meantime, the striking impacts of aluminum additives have also been found in homogeneous catalyst systems which showed better control on the molecular weight of polymers. Carpentier et al. reported that the bimetallic neodymium–magnesium $Nd(allyl)_2Cl(MgCl_2)_2(THF)_4$ combined with TEA or TIBA was highly active and *cis*-1,4-selective for the polymerization of isoprene. Whereas the yttrium

Received: May 13, 2014
Revised: June 27, 2014
Published: July 11, 2014

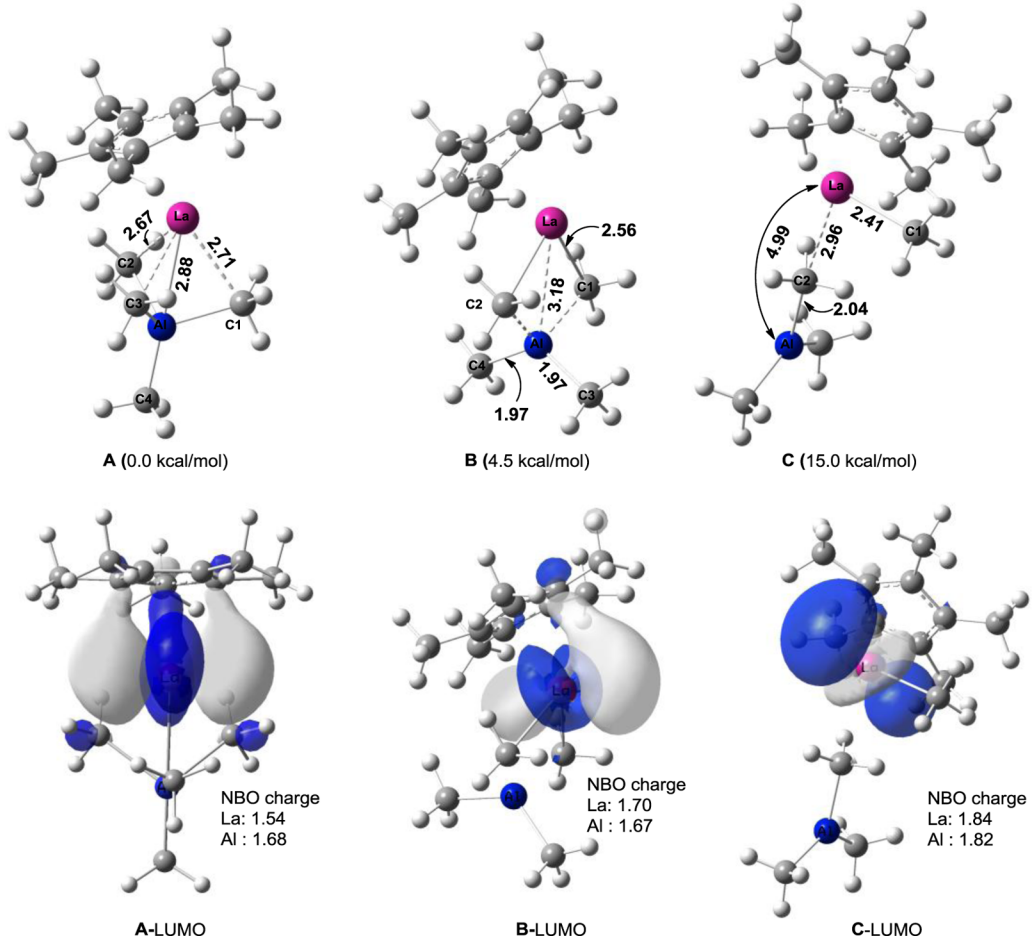

Figure 1. Optimized structures of cationic species **A**, **B**, and **C** (the first row, distances in Å) and their isosurfaces of LUMOs (the second row, isovalue = 0.04). Energies shown are free energy in toluene solution relative to species **A**.

analogue/MAO displaying lower activity enabled the formation of either *cis*-1,4 enriched (75%) or *trans*-1,4 enriched (91%) polyisoprenes, simply replacing the MAO activator by TEA or TIBA, respectively.[4b] Recently, Hou et al. found that the amidinate-ligated yttrium complex $[(NCN_{dipp})Y(o\text{-}CH_2C_6H_4NMe_2)_2]$ (NCN_{dipp} = $PhC(NC_6H_4{}^iPr_2\text{-}2,6)_2$) with 1 equiv of $[Ph_3C][B(C_6F_5)_4]$ showed extremely high activity and excellent 3,4-isotacticity for the isoprene polymerization. However, the addition of TMA shifted dramatically the regio- and stereoselectivity of polymerization from 3,4-isospecificity to *cis*-1,4-selectivity (98%).[5] Compared to *cis*-1,4 polymerization, the *trans*-1,4 polymerization by rare-earth metal has received much less attention owing to few suitable active catalyst systems. Anwander and co-workers reported that half-sandwich heterobimetallic lanthanide/aluminum complexes $[(Cp')Ln(AlMe_4)_2]$ (Cp' = C_5Me_5, C_5Me_4H, $[1,3\text{-}(Me_3Si)_2C_5H_3]$; Ln = rare earth metal) with the activation of borate/borane reagents could catalyze *trans*-1,4-polymerization of isoprene.[6] The highest stereoselectivity was observed for the precatalyst/cocatalyst system $[(C_5Me_5)La(AlMe_4)_2]/B(C_6F_5)_3$ (*trans*-1,4 content: 99.5%, M_w/M_n = 1.18). One interesting question, as mentioned above, is that the Y/Al system by Hou et al. and La/Al system by Anwander give totally different stereospecific polyisoprene. In this respect, the effect of aluminum salts in microstructure-control and molecular weight population should not be ignored. Nevertheless, the related mechanism and factors governing the activity and regio- and stereoselectivity of 1,3-diene polymerization by rare-earth metal complexes in the presence of aluminum reagents have remained to be far from full understanding.[7]

Numerous computational studies[8−12] have been widely and successfully conducted to investigate the mechanism of olefins polymerization catalyzed by group 4 and late transition metal complexes. These theoretical results have effectively promoted the design and development of homogeneous transition metal catalyst. And yet, most of studies focused on mono-olefin polymerization;[8a−c,f,9−11] the polymerization of dienes has remained to be less explored.[8d,12] On the other hand, computational studies on the rare-earth-metal-catalyzed polymerization of dienes are also very limited[13] and are mostly conducted for butadiene polymerization according to the π-allyl-insertion mechanism introduced by Taube et al.[14] There are few examples of computational study on isoprene polymerization catalyzed by the rare-earth-metal complex. Recently, Maron et al. conducted computational studies on the polymerization of conjugated dienes (isoprene was modeled by butadiene) catalyzed by cationic species $[Cp^*ScR]^+$ [13a] and the copolymerization of conjugated dienes (butadiene) with olefins (including 1-hexene) catalyzed by a hemilanthanidocene $[(Cp^*)(BH_4)LnR]$.[13b] We made the primary computational investigation on isoprene polymerization catalyzed by cationic half-sandwich scandium species, in which some complexes and products were optimized.[13c] A series of theoretical calculations of olefin polymerization catalyzed by cationic rare earth metal

dx.doi.org/10.1021/ma500988s | *Macromolecules* 2014, 47, 4596−4606

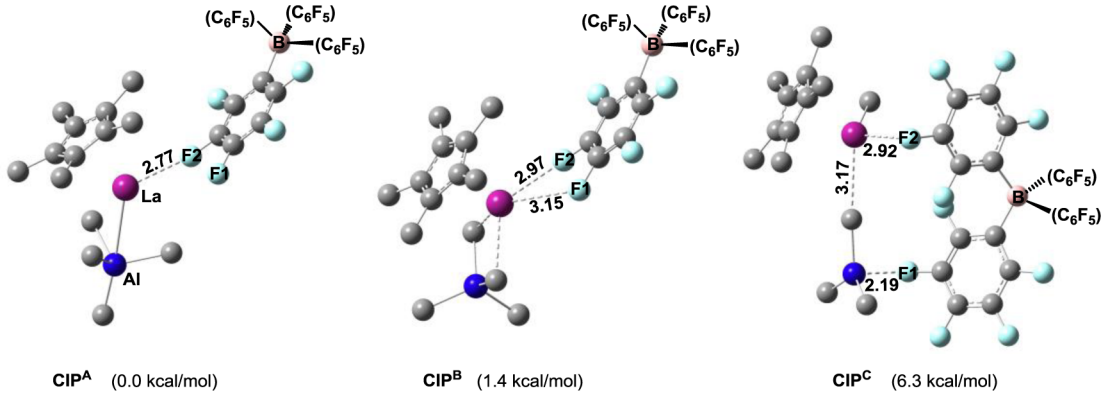

Figure 2. Optimized structures (distance in Å) of contact ion pairs **CIP**^{A}, **CIP**^{B}, and **CIP**^{C}. Energies shown are relative free energies in solution.

complexes were also previously carried out in combination with experimental studies.[13d−h] Recently, we found that the insertion of isoprene into the metal−alkyl bond of a cationic binuclear yttrium complex took place via a kinetically preferable five-center transition state rather than a conventional four-center transition state, which is well-known for the mononuclear-complex-catalyzed alkene polymerization.[13g]

Attracted by the strong correlation of the catalytic performance on the aluminum reagents as well as the sophisticated mechanism of polymerization catalyzed by bimetallic systems, in this work, we focus on the mechanism of *trans*-1,4 (*cis*-1,4) polymerization of isoprene mediated by cationic rare earth and Al heterobimetallic half-sandwich complexes $[(C_5Me_5)Ln(AlMe_4)]^+$(Ln = La and Y). Three objectives are to be addressed in the current theoretical study. The first is to investigate the structure of the active species. The second is to explore the polymerization mechanism of isoprene in La−Al bimetallic systems. The third is to unveil the origin of dramatic difference in the polymerization selectivity between La and Y systems. We hope that the results reported here would give valuable information to the development of more efficient rare-earth-metal polymerization systems.

COMPUTATIONAL DETAILS

All calculations were performed with the Gaussian 09 program.[15] The B3PW91[16] functional was utilized to fully optimize all the stationary points without any symmetry or geometrical constraints. Normal-coordinate analyses were performed to verify the geometrically optimized stationary points and to obtain the thermodynamic data. The 6-31G* basis set was used for C and H atoms, and Al, Y, and La atoms were treated by Stuttgart/Dresden effective core potential (ECP) and the associated basis sets.[17] In the Stuttgart/Dresden ECP used in this study, the most inner 10 electrons of Al and the most inner 28 electrons of Y and La are included in the core. The basis sets of (4s4p)/[2s2p], (8s7p6d)/[6s5p3d], and (14s13p10d8f6g)/[10s8p5d4f3g] were used for Al, Y, and La atoms, respectively. One d-polarization function with exponent of 0.19 was augmented for the Al atom.[18] Such basis sets for geometry optimization are denoted by "BSI". In the NBO analysis, the B3PW91 functional and BSI were applied. To consider the toluene solvation effect, the SMD model[19] developed by Truhlar's group was taken into account by performing B3PW91/BSI single-point calculations on the optimized geometries. Actually, the larger basis set "BSII" (6-31+G** for C, H, and Al atoms and MWB28 together with associated pseudopotential for La and Y atoms) was also used for some calculations of solvation effect, and the obtained relative energy (Figure S4 in Supporting Information) has no significantly change in comparison with that derived from B3PW91/BSI (Figure 5). Therefore, unless otherwise mentioned, the reported free energy in solution was calculated at the level of B3PW91/BSI, including the free energy correction from gas-phase calculation.

RESULTS AND DISCUSSION

Active Species. Four possible bare cationic species $[(C_5Me_5)La(\mu_2\text{-}Me)_3AlMe]^+$ (**A**), $[(C_5Me_5)La(\mu_2\text{-}Me)_2AlMe_2]^+$ (**B**), $[(C_5Me_5)La(Me)(\mu_2\text{-}Me)AlMe_2]^+$ (**C**), and $[(C_5Me_5)La(\mu_2\text{-}Me)AlMe_3]^+$ (**D**) were considered for modeling the initial active species. As shown in Figure 1, the species **B** and **C** are higher in energy than **A** by 4.5 and 15.0 kcal/mol, respectively. Geometrically, the optimized cationic species **A** (Figure 1) with three methyl groups bridging La and Al atoms has La···Al distance of 2.88 Å. The remained methyl group of $AlMe_4$ moiety and two metal atoms (La and Al) almost constructed a nearly linear connection La···Al−CH_3. Optimized species **B** with two bridging methyl groups shows a nearly planar structure constructed by La, Al, and two C atoms of the bridging methyls. In **B**, the distances of La···Al, La···C1 (C2), and La···C3 are 3.18, 2.56, and 4.44 Å, respectively. Unlike **A** and **B**, **C** has a terminal methyl singly bounding to La, and the resulting $AlMe_3$ moiety serves as a neutral ligand coordinating to the La center via a methyl group. There is no direct interaction between La and Al in this species (interatomic distance of 4.99 Å). Attempts to locate species **D** geometrically led to **A** (Figure S1). Further orbital and NBO charge analyses show that the LUMOs of the former three species are dominated by 5d orbital of metal La (contributions of 83.0%, 82.4%, and 85.4% in **A**, **B**, and **C**, respectively), suggesting a feasible access of olefin monomer to the La center. The positive charge on La follows the order of **C** > **B** > **A**, and the charge on Al is also the most positive in **C** than that in **A** and **B**. This suggests that species **C** has stronger Lewis acidity in comparison with the other two species.

Considering the relative stabilities of the three bare cationic species discussed above, we further investigate the stabilities of their corresponding contact ion pairs **CIP**^{A}, **CIP**^{B}, and **CIP**^{C} in solution. Optimized structures of these ion pairs are shown in Figure 2. The anion $[B(C_6F_5)_4]^-$ coordinates with species **A**, **B**, and **C** via one F atom in **CIP**^{A}, two F atoms of a $-C_6F_5$ group in **CIP**^{B}, and two F atoms of two $-C_6F_5$ groups in **CIP**^{C}. Such a structural discrepancy among **CIP**^{A}, **CIP**^{B}, and **CIP**^{C} could be ascribed to the La···Al distance and relatively unsaturated coordination sphere of La and Al centers. The computed relative free energies in toluene solution of these ion pairs suggest that

dx.doi.org/10.1021/ma500988s | *Macromolecules* 2014, 47, 4596−4606

CIP^{C} is less stable than **CIP**^{A} and **CIP**^{B}, and two ion pairs **CIP**^{A} and **CIP**^{B} are nearly isoenergetic with respect to the DFT calculations (Figure 2). On the other hand, the energies required for the separation of ion pairs via coordination of monomer were also calculated. The results indicate that the **C** (30.9 kcal/mol) involved ion pair is more difficult to be separated in comparison with **A** (23.9 kcal/mol) and **B** (21.8 kcal/mol) cases (Scheme 1).

Scheme 1. Separation of Contact Ion Pairs (CIP) via the Coordination of *trans*-Isoprene to La, Generating Isoprene Coordinated Cationic Complex $[C_t]^+$ and Counterion $[B(C_6F_5)_4]^-$

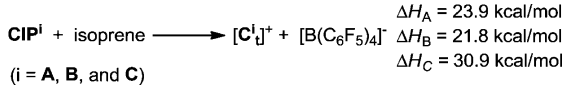

Considering this and the relative stabilities of the bare cations (Figure 1) and their ion pairs (Figure 2), the species **C** is excluded from the initially possible active species at the chain initiation stage. It is noteworthy that an ion pair of **C** coordinated by two F atoms of one $-C_6F_5$ group was found and is higher in energy than **CIP**^{C} by 8.3 kcal/mol (Figure S2 in Supporting Information). Structural comparison of **A** and **B** indicates that the three bridging methyls make the La center of species **A** more crowded and be less favorable for monomer insertion (*vide infra*). This situation together with the relative stabilities discussed above led us to initially choose species **B** as the active species for chain initiation process.

Mechanism of *trans*-1,4-Polymerization. It is generally considered that the η^3-π-allyl insertion mechanism works for the polymerization of conjugated diene catalyzed by transition metal complexes.[8d,14] The coordination of free monomer to the metal center generates prereaction complex. According to the *trans*–*syn* and *cis*–*anti* correlation, there are four conformationally different cationic species with η^3-π-prenyl moiety, viz., supine *syn*-, prone *syn*-, supine *anti*-, and prone *anti*-prenyl, as shown in Figure 3.

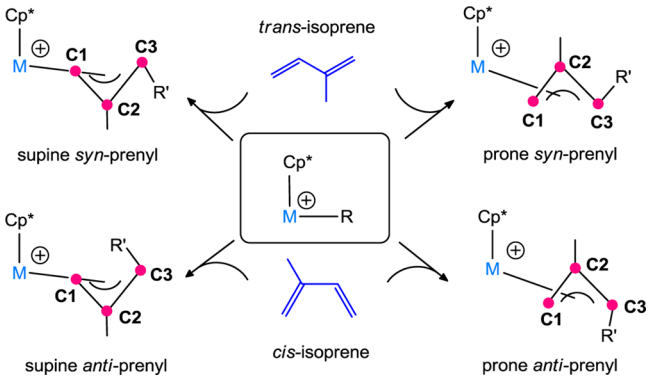

Figure 3. Four possible species with η^3-π-prenyl moiety for chain growth.

Repeated monomer insertion into the η^3-π-allylic prenyl–M linkage implements chain propagation. Therefore, $[(MeC_3H_3R')M(Cp^*)(C_5H_8)]^+$ (M = metal) is regarded as the real active species in the polymerization.[12s] One knows that the consecutive insertion of *trans*-monomer into the allyl–metal bond of active species with *syn*-prenyl moiety and the insertion of *cis*-monomer into the species with *anti*-prenyl moiety are direct pathways leading to *trans*- and *cis*-1,4 unit, respectively (Figure 4). In addition, the isomerization between *anti* and *syn* forms is also possible to occur through a η^1-transition state (Figure 4).

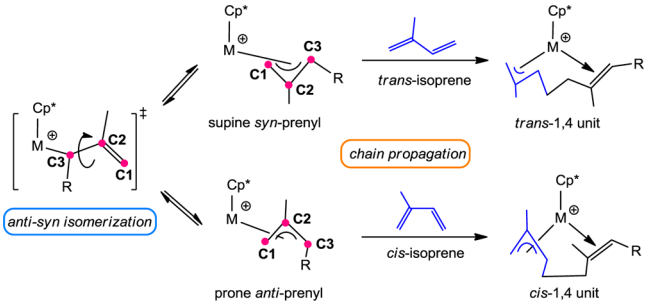

Figure 4. Isomerization of *anti* and *syn* forms and chain propagation.

Thus, the generation of *trans*-1,4 polyisoprene could proceed via two possible pathways, viz., the direct insertion of monomer into *syn*-prenyl species and *anti*–*syn* isomerization prior to monomer insertion. However, it has been found that the *anti*–*syn* isomerization is more difficult than the direct insertion pathways (*vide infra*).

A. Chain Initiation. To access the mechanism working for *trans*-1,4-polymerization of isoprene in the current system, at the chain initiation stage, one needs to investigate the reaction of **B** with isoprene to generate active species with supine or prone η^3-*syn* prenyl moiety (Figure 3).[7d] It is found that the formation of the former species is more kinetically favorable (34.6 kcal/mol) than the latter case (36.7 kcal/mol, see Table S1 in Supporting Information). In the following, the generation of species with supine η^3-*syn*-prenyl moiety is therefore discussed (Figure 5).

In Figure 5, the labeling Coo, TS, and P denote prereaction complex, transition state, and insertion product, respectively. The right superscripts B and C represent active species **B** and **C**, respectively; the subscript t denotes *trans*-monomer insertion; the left superscript Al means the Al–Me bond involved insertion. For example, the **Coo**$^{C}_{t}$ represents species-**C**-based prereaction complex with *trans*-monomer. The reaction of *trans*-isoprene with cation **B** starts with the formation of complex **Coo**$^{B}_{t}$ or ^{Al}**Coo**$^{B}_{t}$. The latter showing an interaction of monomer with both La and Al centers goes through a TS ^{Al}**TS**$^{B}_{t}$ with a rather high energy barrier (43.1 kcal/mol) to give ^{Al}**P**$^{B}_{t}$ via a transfer insertion of terminal Me[2]. The former, **Coo**$^{B}_{t}$, goes through transition state **TS**$^{B}_{t}$ to generate the insertion product **P**$^{B}_{t}$ rather than **P**$^{C}_{t}$ with (μ_2-Me)AlMe$_2$ moiety (see Figure S5 in Supporting Information). This course showing the μ_2-Me[1] transfer insertion overcomes the high energy barrier of 34.6 kcal/mol and is exergonic by −1.4 kcal/mol. These two pathways are hard to kinetically occur with respect to olefin insertion/polymerization. This result shows a good agreement with the finding that the heterobimetallic η^2-complex being similar to species **B** was regarded as a dormant state species in chain transfer polymerization.[20]

To our surprise, however, the **Coo**$^{B}_{t}$ could favorably isomerize to **Coo**$^{C}_{t}$ with one μ_2-Me group and a terminal methyl (Me[1]) connecting to La. This conversion needs to overcome an energy barrier of 22.2 kcal/mol (Figure 5). The **Coo**$^{C}_{t}$ is actually the coordination complex of monomer with cationic species **C**. The compelx **Coo**$^{C}_{t}$ is suitable for the transfer insertion of Me[1] group, and the insertion TS, **TS**$^{C}_{t}$, has been successfully located, giving insertion product **P**$^{C}_{t}$. This insertion process has an energy barrier of 27.2 kcal/mol and is significantly exergonic by −11.2 kcal/mol. Although the prereaction complex **Coo**$^{C}_{t}$ is higher in

dx.doi.org/10.1021/ma500988s | *Macromolecules* 2014, 47, 4596–4606

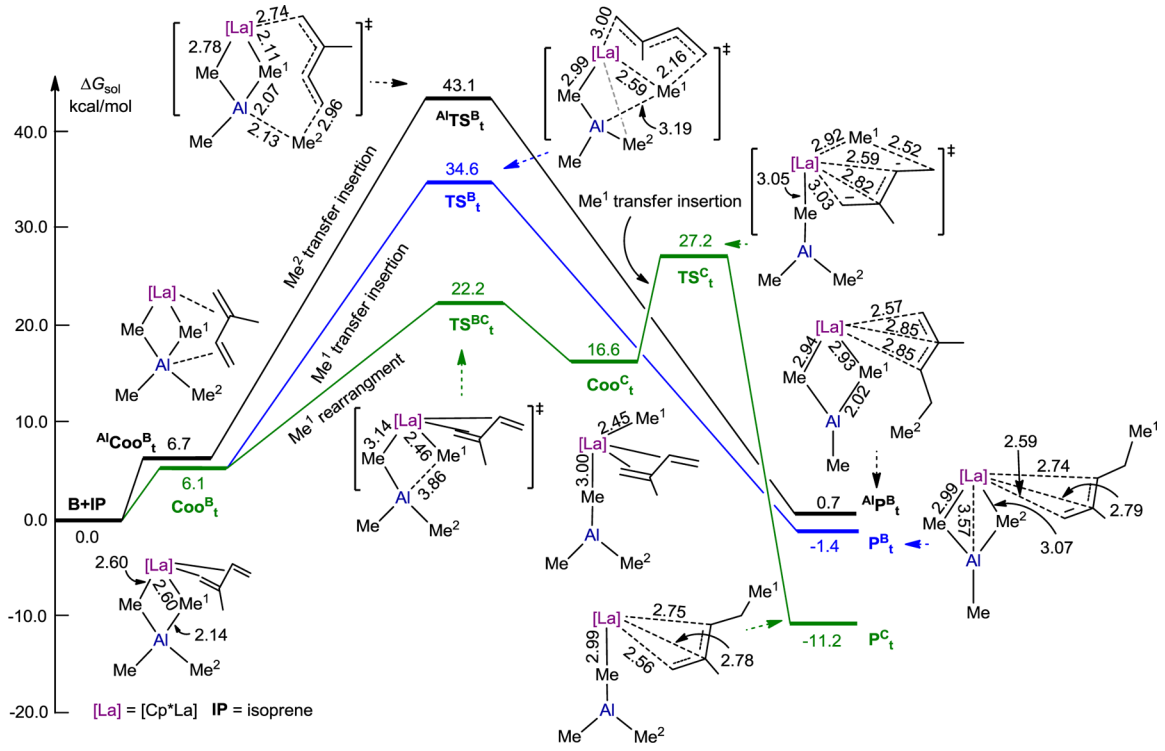

Figure 5. Computed energy profiles (in kcal/mol, free energy in toluene solution, the sign of cation is omitted) for the formation of species with η^3-*syn* prenyl moiety via the reaction of **B** with *trans*-isoprene. The energies given are relative to the energy sum of **B** and one molecule of *trans*-isoprene. Optimized structures of $\mathbf{Coo^B}_t$, $\mathbf{TS^{BC}}_t$, $\mathbf{Coo^C}_t$, $\mathbf{TS^C}_t$, and $\mathbf{P^C}_t$ are shown in Figure S3 of the Supporting Information.

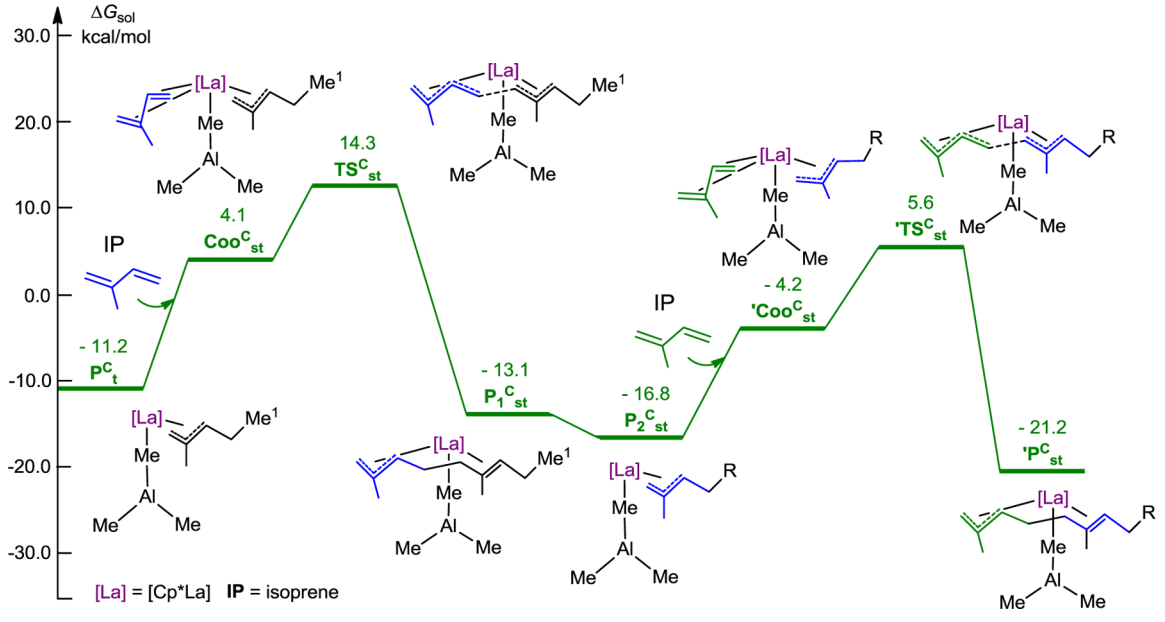

Figure 6. Computed energy profiles (in kcal/mol, free energy in toluene solution, the sign of cation is omitted) for the chain propagation; the energies are relative to the energy sum of **B** and corresponding monomers. The 3D-structures with important geometrical parameters of the stationary points are shown in Figure S9.

energy than $\mathbf{Coo^B}_t$ by 10.5 kcal/mol, the final insertion product $\mathbf{P^C}_t$ is more stable than $\mathbf{Coo^B}_t$ by 17.3 kcal/mol. It is obvious that such an insertion process is significantly favorable both kinetically and thermodynamically in comparison with the pathway though $\mathbf{TS^B}_t$ or $^{Al}\mathbf{TS^B}_t$ (Figure 5). This result suggests that the **C** having one terminal Me as a transfer insertion group and a (μ_2-Me)AlMe$_2$ moiety as a monodentate ligand could be the active cationic species at the chain initiation stage. Actually, a coordination complex of **A** and the monomer has been geometrically optimized, whereas attempts to locate the insertion TS for subsequent transfer insertion of one of the three μ_2-Me groups were fruitless. With the help of relaxed potential energy surface scan, a TS optimization starting with the geometry at the top of scanned curve led to $\mathbf{TS^C}_t$ (see Figure S6 in Supporting Information). This result suggests that the species **A** could be unsuitable for chain initiation.

dx.doi.org/10.1021/ma500988s | *Macromolecules* 2014, 47, 4596−4606

Geometrically, the Me_1 as a transferring insertion group adopts μ_2-manner in $\mathbf{Coo^B}_t$ but is a terminal form in $\mathbf{Coo^C}_t$. This situation makes the former insertion process kinetically less favorable due to the cleavages of both La−Me_1 and Al−Me_1 bonds in comparison with the latter case undergoing only the cleavage of La−Me_1 bond. This could account for the higher relative energy of $\mathbf{TS^B}_t$ compared with $\mathbf{TS^C}_t$ (Figure 5). It is noted that the insertion product $\mathbf{P^B}_t$ with one terminal- and two μ_2-Me groups is less stable than the $\mathbf{P^C}_t$ with two terminal- and one μ_2-Me groups. To get better understanding on the relative stability of the $\mathbf{P^C}_t$ in comparison with $\mathbf{P^B}_t$, energy decomposition analyses were performed. For this purpose, single-point energies were calculated for the fragments of $[La]AlMe_3$ ($[La] = [Cp^*La]^{2+}$) and $[\eta^3\text{-}C_5H_8Me]^-$ with their geometries in $\mathbf{P^C}_t$ and $\mathbf{P^B}_t$, respectively. It was found that the $[La]AlMe_3$ moiety in $\mathbf{P^C}_t$ is lower in energy than that in $\mathbf{P^B}_t$ by 4.9 kcal/mol and the η^3-C_5H_8Me moiety in $\mathbf{P^C}_t$ is only 0.2 kcal/mol higher than that in $\mathbf{P^B}_t$. The interaction energy between the two moieties is also lower in the former case (−129.6 kcal/mol for $\mathbf{P^C}_t$ vs −128.4 kcal/mol for $\mathbf{P^B}_t$). These results suggest that the less stability of $\mathbf{P^B}_t$ could be ascribed to the higher energy of its $[La]AlMe_3$ moiety and weaker interaction between $[La]AlMe_3$ and η^3-C_5H_8Me moieties in comparison with the case of $\mathbf{P^C}_t$.

B. Chain Propagation. In view of the result that the formation of $\mathbf{P^C}_t$ is more both kinetically and thermodynamically favorable compared with $\mathbf{P^B}_t$, the former was considered for the subsequent monomer insertion event. To model the prereaction complex during the chain propagation, the frontier orbital analysis of $\mathbf{P^C}_t$ has been performed. It is found that the LUMO of $\mathbf{P^C}_t$ is predominated by La-5d (76.5%) and the contribution of Al-3p orbital is minor (0.7%, Figure S7). This suggests that the incoming monomer could preferably coordinate to the La center.

As shown in Figure 6, after the formation of the prereaction complex $\mathbf{Coo^C}_{st}$ showing a coordination of the monomer to La center of $\mathbf{P^C}_t$, the insertion of isoprene occurs through the transition state $\mathbf{TS^C}_{st}$ and then leads to the insertion product $\mathbf{P_1}^{\mathbf{C}}_{st}$. This insertion process, which overcomes a free energy barrier of 25.5 kcal/mol (relative to $\mathbf{P^C}_t$), is exergonic by 1.9 kcal/mol (relative to $\mathbf{P^C}_t$). Similarly, the insertion of the third monomer could take place via the coordination of the incoming isoprene to the $\mathbf{P_2}^{\mathbf{C}}_{st}$ which was derived from $\mathbf{P_1}^{\mathbf{C}}_{st}$ via a thermodynamically feasible chain rotation. The newly formed coordination complex $'\mathbf{C^C}_{st}$ goes through transition state $'\mathbf{TS^C}_{st}$ to give product $'\mathbf{P^C}_{st}$. It is found that these two transition states ($\mathbf{TS^C}_{st}$ and $'\mathbf{TS^C}_{st}$) are structurally similar, and the chain growth could smoothly occur. It is noteworthy that the coordination of the incoming monomer to both La and Al centers of $\mathbf{P^C}_t$ and $\mathbf{P^B}_t$ and subsequent insertion is less energetically favorable in comparison with the corresponding process shown in Figure 6 (see Figure S8).

Selectivity. For better understanding of the origin of highly selective polymerization of isoprene, it is necessary to make a comparison in details for *trans*-1,4 and *cis*-1,4 polymerizations. A number of computational studies[8d,12] indicate that the stereoselectivity of 1,3-diene polymerization mainly depends on the configuration of the coordinated monomer and the isomerization between *syn*- and *anti*-modes. All the insertion processes in the current work follow the π-allyl-insertion mechanism proposed by Taube et al.[14]

As discussed above, the chain initiation and propagation actually occur through one CH_3-bridged La/Al bimetallic cationic species such as **C**, and the insertion event preferably takes place at the La center. Therefore, the cationic species **C** and $\mathbf{P^C}_t$ were considered for the investigation of selectivity. There are two manners (*trans* vs *cis*) for isoprene to coordinate to the La center of cationic species **C**. The chain initiation occurs through the coordinations and subsequent insertions of *trans*-isoprene and *cis*-isoprene into the La−Me bond of species **C** to give products with the *syn*-η^3- and *anti*-η^3-allylic moieties, respectively. The corresponding relative energies are shown in Table 1.

Table 1. Computed Free Energies in Toluene Solution (kcal/mol, Relative to B and Monomer) for the Insertion of *trans*- and *cis*-Isoprene into La−Me Bond of Species C at the Chain Initiation Stage[a]

insertion modes[b]	$\mathbf{Coo^C}$	$\mathbf{TS^C}$	$\mathbf{P^C}$
trans-isoprene(*si*)[c]	16.6 ($\mathbf{Coo^C}_t$)	27.2 ($\mathbf{TS^C}_t$)	−11.2 ($\mathbf{P^C}_t$)
cis-isoprene(*si*)	19.4 ($\mathbf{Coo^C}_c$)	28.6 ($\mathbf{TS^C}_c$)	−8.0 ($\mathbf{P^C}_c$)

[a]See Table S1 in the Supporting Information for other unfavorable insertion modes (refs 12u and v). [b]Denoting *si*-insertion of *trans*- and *cis*-isoprene, respectively. It is similar for that in Table 2. [c]Data taken from Figure 5.

It has been found that the *trans*-isoprene is easier to coordinate with metal center than *cis*-isoprene (complexation energies of 16.6 vs 19.4 kcal/mol), and the subsequent insertion is also more favorable for the *trans* case with respect to the relative energies of TSs ($\mathbf{TS^C}$) and products ($\mathbf{P^C}$, Table 1).

Therefore, the *trans*-isoprene induced product $\mathbf{P^C}_t$ with *syn*-η^3-allylic moiety is preferred at the chain initiation stage. Geometrically, the transition state $\mathbf{TS^C}_t$ with *trans*/*syn* configuration shows a η^3-coordination mode, while the $\mathbf{TS^C}_c$ with *cis*/*anti* configuration shows a η^4-coordination manner (Figure 7). To further explore the stereoselectivity of isoprene polymerization, the chain propagation has also been compared.

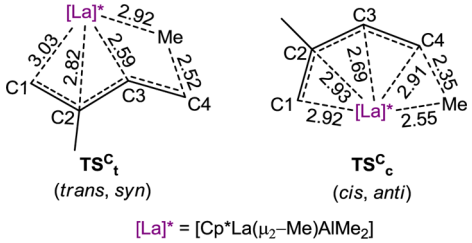

Figure 7. Schematic representation (distances in Å) of the transition states $\mathbf{TS^C}_t$ and $\mathbf{TS^C}_c$. The ligands including $AlMe_3$ were replaced by [La]* for clarity, and the sign of cation is omitted.

As shown in Scheme 2a, the coordinating complexes $\mathbf{Coo^C}_{st}$ and $\mathbf{Coo^C}_{at}$ formed via coordination of *trans*-isoprene to the $\mathbf{P^C}_t$ with *syn*-configuration and to the $\mathbf{P^C}_c$ with *anti*-configuration, respectively, serve as active species for the productive enchainment cycles.[12s] Chain propagation could go through the $\mathbf{Coo^C}_{st} \rightarrow \mathbf{TS^C}_{st} \rightarrow \mathbf{P^C}_{st}$ or $\mathbf{Coo^C}_{at} \rightarrow \mathbf{TS^C}_{at} \rightarrow \mathbf{P^C}_{at}$ pathway. Similarly, as shown in Scheme 2b, the *cis*-isoprene-participated chain propagation follows $\mathbf{Coo^C}_{sc} \rightarrow \mathbf{TS^C}_{sc} \rightarrow \mathbf{P^C}_{sc}$ or $\mathbf{Coo^C}_{ac} \rightarrow \mathbf{TS^C}_{ac} \rightarrow \mathbf{P^C}_{ac}$.

It has been found that the *trans*-isoprene coordinated complex $\mathbf{Coo^C}_{st}$ is more stable than *cis*-isoprene coordinated complex $\mathbf{Coo^C}_{ac}$. The $\mathbf{Coo^C}_{st}$ overcomes an energy barrier of 10.2 kcal/mol to yield the most stable *trans*-1,4 unit product $\mathbf{P^C}_{st}$ having lowest energy of −17.1 kcal/mol among the four products ($\mathbf{P^C}_{st}$, $\mathbf{P^C}_{at}$, $\mathbf{P^C}_{sc}$, and $\mathbf{P^C}_{ac}$) shown in Scheme 2. Therefore, the process $\mathbf{Coo^C}_{st} \rightarrow \mathbf{TS^C}_{st} \rightarrow \mathbf{P^C}_{st}$ is the most favorable pathway in

dx.doi.org/10.1021/ma500988s | *Macromolecules* 2014, 47, 4596−4606

Scheme 2. Computed Energy Profiles (in kcal/mol, Free Energy in Toluene Solution, the Sign of Cation Is Omitted) for Isoprene 1,4-Polymerization with $[(C_5Me_5)La(\mu_2\text{-}Me)AlMe_2(\eta^3\text{-}C_6H_{11})]^+$ as the Active Species[a]

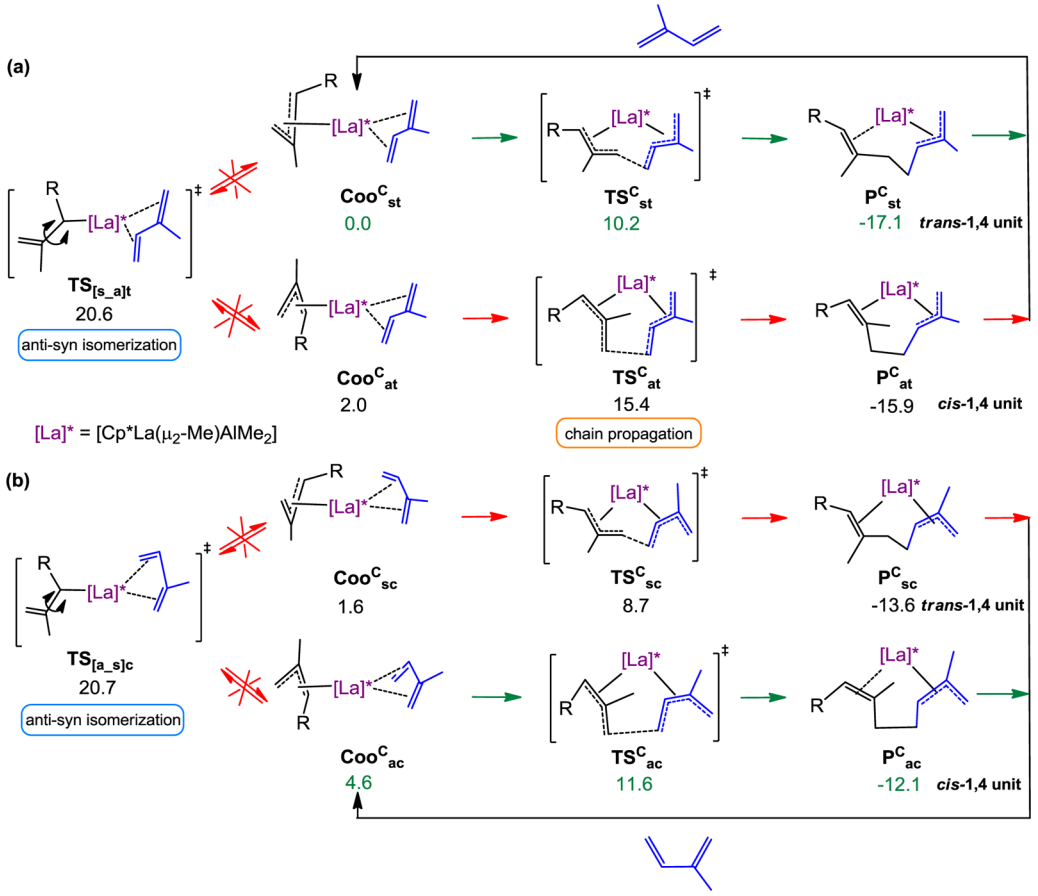

[a]The labeling Coo, TS, and P denote prereaction complex, transition state, and insertion product, respectively; the superscript C represents active species **C**; the subscripts st, at, sc, and ac denote *syn/trans*, *anti/trans*, *syn/cis*, and *anti/cis* configuration, respectively. For example, the $\mathbf{Coo^C_{st}}$ represents species-**C**-based prereaction complex with *syn/trans* configuration. Other unfavorable transition states with various orientations of the allyl group and the incoming monomer, as the isomers of $\mathbf{TS^C_{st}}$ and $\mathbf{TS^C_{ac}}$, are shown in Table S2.

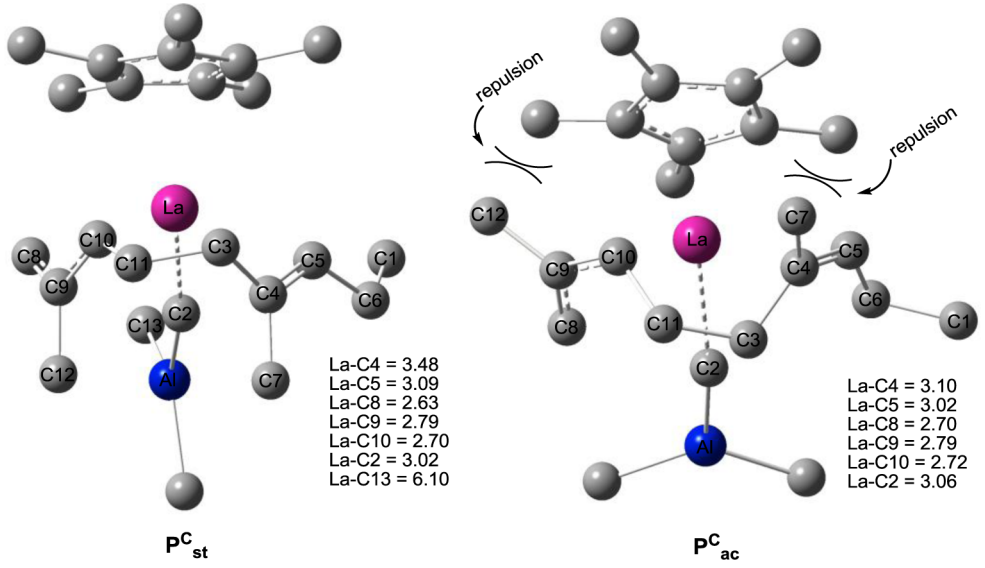

Figure 8. Geometric structures (distances in Å) for products $\mathbf{P^C_{st}}$ and $\mathbf{P^C_{ac}}$. The hydrogen atom and the bonding between La and the growing chain were omitted for clarity. La···C13 distance of 6.10 Å in $\mathbf{P^C_{st}}$ suggesting no bonding between the two atoms.

thermodynamics, which is consistent with the experimental observation[6] and the previous result that the *trans*-1,4-polyisoprene is a thermodynamic product.[13a] It is noteworthy that an alternative pathway $\mathbf{Coo^C_{sc}} \rightarrow \mathbf{TS^C_{sc}} \rightarrow \mathbf{P^C_{sc}}$ also giving

dx.doi.org/10.1021/ma500988s | *Macromolecules* 2014, 47, 4596−4606

trans-1,4 polymer shows the lowest energy barrier of 8.7 kcal/mol. Nevertheless, an *anti*−*syn* regulation (via transition state $\mathbf{TS}_{[a\_s]c}$) would be required prior to the next loop of $\mathbf{Coo}^{C}_{sc} \rightarrow \mathbf{TS}^{C}_{sc} \rightarrow \mathbf{P}^{C}_{sc}$. By contrast, the *anti*−*syn* isomerization needs to surmount the higher energy barrier (20.7 kcal/mol) than that for the direct C−C bond formation along with $\mathbf{Coo}^{C}_{ac} \rightarrow \mathbf{TS}^{C}_{ac} \rightarrow \mathbf{P}^{C}_{ac}$, leading to product $\mathbf{P}^{C}_{ac}$ (an energy barrier of 11.6 kcal/mol, Scheme 2b). However, this pathway is kinetically and thermodynamically less favorable in comparison with the formation of product $\mathbf{P}^{C}_{st}$ with *trans*-1,4 unit via the $\mathbf{Coo}^{C}_{st} \rightarrow \mathbf{TS}^{C}_{st} \rightarrow \mathbf{P}^{C}_{st}$ pathway (Scheme 2a). Such kinetic and thermodynamic priorities for the formation of *trans*-1,4 unit were also suggested by the results derived from MPW1K and BP86 functionals (see Table S3 in Supporting Information).

For a better understanding of the thermodynamic priority for the formation of *trans*-1,4 product, the geometrical structures of $\mathbf{P}^{C}_{ac}$ and $\mathbf{P}^{C}_{st}$ have been compared. As shown in Figure 8, in the $\mathbf{P}^{C}_{ac}$, there is steric repulsion between the Cp* ligand and the methyl groups of the inserted η^3-prenyl units, while such repulsion is absent in $\mathbf{P}^{C}_{st}$. This could account for the more stability of the latter. The same is true for the corresponding coordination complexes of $\mathbf{Coo}^{C}_{ac}$ and $\mathbf{Coo}^{C}_{st}$. Further energy decomposition analysis indicates that the less deformations of the isoprene moiety and its counterparts also account for the more stability of $\mathbf{Coo}^{C}_{st}$ in comparison with $\mathbf{Coo}^{C}_{ac}$. It is noteworthy that the $AlMe_3$ constructed plane in the $\mathbf{P}^{C}_{st}$ is perpendicular to the growing chain due to the steric effect of methyl groups of prenyl unit, whereas such a plane is parallel to the growing chain in $\mathbf{P}^{C}_{ac}$. The free rotation of the $AlMe_3$ ligand around the La−$MeAlMe_2$ bond axis should be beneficial to such an orientation adaptation of $AlMe_3$ ligand.

***Cis*-1,4-polymerization of Isoprene by Analogous Yttrium System.** One interesting question is that, unlike the La−Al catalyst system, the Y analogue tends to produce *cis*-1,4 polyisoprene. To uncover the origin of the experimentally observed different stereoselectivity, the chain initiation and propagation steps promoted by the Y analogue $[(C_5Me_5)YMe(\mu_2\text{-}Me)AlMe_2)]^+$ ($\mathbf{C_Y}$) have been also investigated.

Table 2 shows the computed relative energies for the chain initiation stage, viz., the insertion process of isoprene into Y−Me bond of $\mathbf{C_Y}$. As shown in this table, the insertion of *trans*-isoprene is kinetically less favorable by 1.4 kcal/mol, but the resulting *syn*-η^3-allyl product is energetically more stable by 3.3 kca/mol in comparison with *cis*-isoprene insertion giving *anti*-η^3-allyl product. This suggests that the *syn*-η^3-prenyl and *anti*-η^3-prenyl products are the thermodynamically and kinetically controlled products, respectively.

Table 2. Computed Free Energies in Solution (in kcal/mol) for the Insertion of Isoprene (*trans*- and *cis*-Forms) into Y−Me Bond of $\mathbf{C_Y}$ (Energies Are Relative to the Energy Sum of *trans*-Isoprene and $\mathbf{C_Y}$)[a]

insertion modes	coordination complex ($\mathbf{Coo}^{CY}$)	transition state ($\mathbf{TS}^{CY}$)	insertion product ($\mathbf{P}^{CY}$)
trans-isoprene(*si*)	8.7 ($\mathbf{Coo}^{CY}_{t}$)	19.3 ($\mathbf{TS}^{CY}_{t}$)	−17.6 ($\mathbf{P}^{CY}_{t}$)
cis-isoprene(*si*)	9.0 ($\mathbf{Coo}^{CY}_{c}$)	17.9 ($\mathbf{TS}^{CY}_{c}$)	−14.3 ($\mathbf{P}^{CY}_{c}$)

[a]See Table S4 in the Supporting Information for other unfavorable insertion modes (refs12u and v).

In the chain propagation as indicated in Table 3, *cis*-isoprene insertion process overcomes a free energy barrier of 25.7 kcal/mol and is endergonic by 0.5 kcal/mol. However, the *trans*-isomer insertion needs to overcome a free-energy barrier of 22.0 kcal/mol and is exergonic by −4.9 kcal/mol. Both the prereaction complex ($\mathbf{Coo}^{CY}_{st}$) and transition state ($\mathbf{TS}^{CY}_{st}$) for *trans*-isoprene insertion are lower in energy than those for *cis*-isoprene insertion by 2.7 and 3.7 kcal/mol, respectively. And *trans*-isoprene insertion product $\mathbf{P}^{CY}_{st}$ is also stable than the *cis*-isoprene insertion $\mathbf{P}^{CY}_{ac}$. Thus, the *trans*-isoprene insertion is more kinetically and thermodynamically favorable. Nevertheless, this result is inconsistent with the experimental result showing dominant *cis*-1,4 selectivity.

To clarify this descrepancy, a further analysis of energy decomposition of $\mathbf{TS}^{CY}_{st}$ and $\mathbf{TS}^{CY}_{ac}$ was carried out. We define the isoprene moiety in these transition states as fragment F1 and the remained part as fragment F2. The energies of the fragments F1 and F2 at the geometry they have in the $\mathbf{TS}^{CY}_{st}$ (or in $\mathbf{TS}^{CY}_{ac}$) were evaluated through single-point calculations. These single-point energies, together with the energy of the respective fragments in their optimized geometry, allow for the estimation of the deformation energies of the two fragments, $\Delta E_{def}(F1)$ and $\Delta E_{def}(F2)$. Such single-point energies of the fragments and the electronic energy of TS were used to estimate the interaction energy ΔE_{int} (corrected by basis set superposition error, BSSE) between F1 and F2 fragments. As the energy of the TS, ΔE_{TS}, is evaluated with respect to the energy of the two separated fragments, the relation $\Delta E_{TS} = \Delta E_{int} + \Delta E_{def}(F1) + \Delta E_{def}(F2)$ holds. The following results were found for $\mathbf{TS}^{CY}_{st}$: $\Delta E_{int} = -31.6$ kcal/mol, $\Delta E_{def}(F1) = 12.2$ kcal/mol, $\Delta E_{def}(F2) = 20.2$ kcal/mol, and therefore $\Delta E_{TS} = 0.9$ kcal/mol. While the results of energy decomposition for $\mathbf{TS}^{CY}_{ac}$ are $\Delta E_{int} = -36.2$ kcal/mol, $\Delta E_{def}(F1) = 15.7$ kcal/mol, $\Delta E_{def}(F2) = 21.9$ kcal/mol, and therefore $\Delta E_{TS} = 1.4$ kcal/mol. The ΔE_{int} value of 0.9 kcal/mol for $\mathbf{TS}^{CY}_{st}$ is lower than that for $\mathbf{TS}^{CY}_{ac}$ by 1.4 kcal/mol. It is obvious that the total deformation energy ΔE_{def} of 37.6 (21.9 + 15.7) kcal/mol in $\mathbf{TS}^{CY}_{ac}$ shields the superiority of strong interaction (−36.2 kcal/mol) between F1 and F2 fragments in $\mathbf{TS}^{CY}_{ac}$ and further makes this TS less stable. On the basis of this result, we speculated that the observed *cis*-1,4-polymerization in the Y complex system could occur under the situation of less steric hindrance and that the $AlMe_3$ ligand might departed from the Y metal center during isoprene polymerization. Therefore, we made further calculations on chain propagation promoted by $[(C_5Me_5)Y(C_6H_{11})]^+$ species without the $AlMe_3$ ligand. The results are shown in Table 3. As expected, the *cis*-isoprene insertion process leading to *cis*-product overcomes an energy barrier of 8.6 kcal/mol and is exergonic by 12.5 kcal/mol, whereas the *trans*-insertion process leading to *trans*-product $'\mathbf{P}^{CY}_{st}$ is less kinetically favorable (11.5 vs 8.6 kcal/mol). This result is in line with the experimental observation that the *cis*-1,4-selective polymerization was favored in the Y complex system. Unlike the case of $\mathbf{TS}^{CY}_{ac}$ and $\mathbf{TS}^{CY}_{st}$, the total deformation energies in the $AlMe_3$-free TSs, viz., $'\mathbf{TS}^{CY}_{ac}$ and $'\mathbf{TS}^{CY}_{st}$, are almost same (28.5 and 29.9 kcal/mol, respectively), as suggested by further energy decomposition analyses. Therefore, it is proposed that the $AlMe_3$ ligand could depart from Y center during isoprene polymerization to produce *cis*-1,4-polyisoprene. For better understanding of such a behavior of $AlMe_3$ ligand, the dissociation free energies of $AlMe_3$ in the TSs $\mathbf{TS}^{CY}_{ac}$ and $\mathbf{TS}^{CY}_{st}$ (Table 3) were calculated at the level of M06-D3[21] with dispersion correction. To get more reliable dissociation energies of $AlMe_3$, the BSSE and D3 dispersion corrections were considered. It has been found that the calculated dissociation free energies are −7.3 and −1.0 kcal/mol for the case of $\mathbf{TS}^{CY}_{ac}$

dx.doi.org/10.1021/ma500988s | *Macromolecules* 2014, 47, 4596−4606

Table 3. Computed Relative Free Energies in Toluene Solution (kcal/mol) for Chain Propagation Promoted by Y Complexes with and without $AlMe_3$ Ligand (Energies Are Relative to $'Coo^{CY}_{st}$)[a]

active species	insertion mode[b]	Coo^{CY}	TS^{CY}	P^{CY}
$[(C_5Me_5)Y(syn\text{-}\eta^3\text{-}C_6H_{11})(\mu_2\text{-}Me)AlMe_2)]^+$	*trans*-isoprene(*si*)-*syn*	14.7 (Coo^{CY}_{st})	22.0 (TS^{CY}_{st})	−4.9 (P^{CY}_{st})
$[(C_5Me_5)Y(anti\text{-}\eta^3\text{-}C_6H_{11})(\mu_2\text{-}Me)AlMe_2)]^+$	*cis*-isoprene(*si*)-*anti*	17.4 (Coo^{CY}_{ac})	25.7 (TS^{CY}_{ac})	0.5 (P^{CY}_{ac})
$[(C_5Me_5)Y(syn\text{-}\eta^3\text{-}C_6H_{11})]^+$	*trans*-isoprene(*si*)-*syn*	0.0 ($'Coo^{CY}_{st}$)	11.5 ($'TS^{CY}_{st}$)	−12.7 ($'P^{CY}_{st}$)
$[(C_5Me_5)Y(anti\text{-}\eta^3\text{-}C_6H_{11})]^+$	*cis*-isoprene(*si*)-*anti*	4.1 ($'Coo^{CY}_{ac}$)	8.6 ($'TS^{CY}_{ac}$)	−12.5 ($'P^{CY}_{ac}$)

[a]See Table S5 in the Supporting Information for other unfavorable insertion modes (refs12u and v). [b]For example, the *trans*-isoprene(*si*)-*syn* denotes the *si*-insertion of *trans*-isoprene into the species with *syn*-moiety.

and TS^{CY}_{st}, respectively (Table S6 in Supporting Information). This result suggests that the dissociation of $AlMe_3$ in TS^{CY}_{ac} is a significantly exergonic process during the chain propagation and is therefore favorable to give $'TS^{CY}_{ac}$ (Table 3) to achieve *cis*-1,4-polymerization. For a comparison, such dissociation free energies were also calculated for the corresponding TSs involved in the La system, viz., TS^{C}_{ac} and TS^{C}_{st} (Scheme 2), and the free energies of −1.9 and 0.1 kcal/mol were found for the cases of TS^{C}_{ac} and TS^{C}_{st}, respectively (Table S6). This suggests a less favorable dissociation process in comparison with the case of TS^{CY}_{ac} (−7.3 kcal/mol). Considering that DFT methods might fail to describe bridging Al alkyls and that the MPW1K functional was reported to be comparable to multireference methods,[22] the MPW1K functional was also used. The result and that from B3PW91-D3 also indicate more favorable dissociation of $AlMe_3$ in the case of TS^{CY}_{ac} compared with other three TSs (Table S6). This is not surprising since La has bigger ionic radius (1.36 Å) and larger general coordination number (12) than that of atom Y (ionic radius of 1.08 Å and coordination number of 9).[23] Therefore, the $AlMe_3$ ligand plays a key role in regulating the stereoselective polymerization of isoprene in the system studied.

CONCLUSION

In conclusion, the mechanistic details of *trans*-1,4 polymerization of isoprene by cationic species $[(C_5Me_5)La(AlMe_4)]^+$ have been theoretically disclosed here. Three possible bare active species $[(C_5Me_5)La(\mu_2\text{-}Me)_3AlMe]^+$ (**A**), $[(C_5Me_5)La(\mu_2\text{-}Me)_2AlMe_2]^+$ (**B**), and $[(C_5Me_5)La(Me)(\mu_2\text{-}Me)AlMe_2]^+$ (**C**) as well as their corresponding contacting ion pairs with $[B(C_6F_5)_4]^-$ counterion have been structurally optimized. In comparison, species **A** and **B** are more stable than species **C**, and the **C** shows stronger interaction with counterion $[B(C_6F_5)_4]^-$ in comparison with other two species. The isoprene-coordinated complexes Coo^{A}_{t}, Coo^{B}_{t}, and Coo^{C}_{t} have also been located for bare species **A**, **B**, and **C**, respectively. Kinetically, the chain initiation promoted by Coo^{B}_{t} is less favorable than the transformation from Coo^{B}_{t} to Coo^{C}_{t}, and the chain initiation promoted by Coo^{A}_{t} failed because of big steric hindrance around La center. The chain initiation promoted by complex Coo^{C}_{t} has relatively lower energy barrier and the **C** could be the true active species for chain initiation. During the chain propagation, the monomer insertion achieving *trans*-1,4 polymer occurs at La center of Coo^{C}_{t} with $AlMe_3$ moiety as a ligand, whereas La/Al bimetal-cooperated monomer insertion pathways have been found to be unfavorable. The current calculation results indicate that the experimentally observed *trans*-1,4 stereoselectivity is under thermodynamic control. Interestingly, in the Y analogous system, the $AlMe_3$ ligand tends to go away from the Y center during the chain propagation, which results in a more favorable process producing *cis*-1,4 polyisoprene. This discrepancy could be ascribed to the larger ionic radius of La and less favorable dissociation of $AlMe_3$ moiety from the La center in comparison with the case of analogous Y system. Having achieved good agreement with experimental results, it is proposed that the $AlMe_3$ moiety serves as a ligand coordinating to La center via one of the three Me groups during the La-catalyzed *trans*-1,4-polymerization of isoprene, but it dissociates from the rare earth metal center in the analogous Y system producing *cis*-1,4-polymer, suggesting a crucial role of the $AlMe_3$ moiety in the regulation of stereoselectivity in such polymerization systems.

ASSOCIATED CONTENT

Supporting Information

Figures giving the energy profiles calculated in solution by using larger basis set and La/Al bimetal-cooperated monomer insertion, optimizing processes for P^{B}_{t} and possible species **D**, another geometric structures for an ion pair of **C**, the relaxed PES scan, and the optimized structures in the most favorable pathway; and tables providing the energy profiles of all chain initiation processes based on species **B** and **C**, the comparison of selectivity in chain propagation computed at the levels of BP86 and MPW1K, the optimized Cartesian coordinates, total energies, and the imaginary frequencies of TSs. This material is available free of charge via the Internet at http://pubs.acs.org.

AUTHOR INFORMATION

Corresponding Author

*E-mail: luoyi@dlut.edu.cn (Y.L.).

Notes

The authors declare no competing financial interest.

ACKNOWLEDGMENTS

This work was supported by the NSFC (No. 21174023, 21137001). Y.L. thanks the Fundamental Research Funds for the Central Universities (DUT13ZD103). The authors also thank RICC (RIKEN Integrated Cluster of Clusters) and the Network and Information Center of Dalian University of Technology for part of computational resources.

REFERENCES

(1) Porri, L.; Giarrusso, A. In *Comprehensive Polymer Science*; Eastmond, C., Ledwith, A., Russo, S., Sigwalt, P., Eds.; Pergamon: Oxford, 1989; Vol. 4, pp 53−108.

(2) (a) Kent, E. G.; Swinney, F. B. *Ind. Eng. Chem. Prod. Res. Dev.* **1966**, *5*, 134−138. (b) Zhang, Z.; Cui, D.; Wang, B.; Liu, B.; Yang, Y. *Struct. Bonding (Berlin)* **2010**, *137*, 49−108.

(3) Ricci, G.; Sommazzi, A.; Masi, F.; Ricci, M.; Boglia, A.; Leone, G. *Coord. Chem. Rev.* **2010**, *254*, 661−676.

(4) (a) Dong, W.; Masuda, T. *J. Polym. Sci., Part A: Polym. Chem.* **2002**, *40*, 1838−1844. (b) Ajellal, N.; Furlan, L.; Thomas, C. M.; Casagrande, O. L., Jr.; Carpentier, J. F. *Macromol. Rapid Commun.* **2006**, *27*, 338−343.

(5) Zhang, L.; Nishiura, M.; Yuki, M.; Luo, Y.; Hou, Z. *Angew. Chem., Int. Ed.* **2008**, *47*, 2642−2645.

(6) (a) Zimmermann, M.; Törnroos, K. W.; Anwander, R. *Angew. Chem., Int. Ed.* **2008**, *47*, 775−778. (b) Zimmermann, M.; Törnroos, K. W.; Sitzmann, H.; Anwander, R. *Chem.—Eur. J.* **2008**, *14*, 7266−7277. (c) Zimmermann, M.; Volbeda, J.; Törnroos, K. W.; Anwander, R. *C. R. Chim.* **2010**, *13*, 651−660.
(7) Li, X.; Wang, X.; Tong, X.; Zhang, H.; Chen, Y.; Liu, Y.; Liu, H.; Wang, X.; Nishiura, M.; He, H.; Lin, Z.; Zhang, S.; Hou, Z. *Organometallics* **2013**, *32*, 1445−1458.
(8) For reviews, see: (a) Rappe, A. K.; Skiff, W. M.; Casewit, C. J. *Chem. Rev.* **2000**, *100*, 1435−1456. (b) Niu, S.; Hall, M. B. *Chem. Rev.* **2000**, *100*, 353−406. (c) Michalak, A.; Ziegler, T. In *Computational Modeling of Homogeneous Catalysis*; Feliu, M., Agusti, L., Eds.; Kluwer: Dordrecht, The Netherlands, 2002; Vol. 25, pp 57−78. (d) Tobisch, S. *Acc. Chem. Res.* **2002**, *35*, 96−104. (e) Bo, C.; Maseras, F. *Dalton Trans.* **2008**, 2911−2919. (f) Mandal, S. K.; Roesky, H. W. *Acc. Chem. Res.* **2010**, *43*, 248−259.
(9) For examples, see: (a) Woo, T. K.; Ziegler, T. *Organometallics* **1994**, *13*, 2252−2261. (b) Xu, Z.; Vanka, K.; Firman, T.; Michalak, A.; Zurek, E.; Zhu, C.; Ziegler, T. *Organometallics* **2002**, *21*, 2444−2453. (c) Flisak, Z.; Ziegler, T. *Macromolecules* **2005**, *38*, 9865−9872. (d) Margl, P.; Deng, L.; Ziegler, T. *J. Am. Chem. Soc.* **1998**, *120*, 5517−5525. (e) Froese, R. D. J.; Musaev, D. G.; Morokuma, K. *Organometallics* **1999**, *18*, 373−379. (f) Froese, R. D. J.; Musaev, D. G.; Matsubara, T.; Morokuma, K. *J. Am. Chem. Soc.* **1997**, *119*, 7190−7196. (g) Musaev, D. G.; Froese, R. D. J.; Svensson, M.; Morokuma, K. *J. Am. Chem. Soc.* **1997**, *119*, 367−374. (h) Froese, R. D. J.; Musaev, D. G.; Morokuma, K. *J. Am. Chem. Soc.* **1998**, *120*, 1581−1587. (i) Yoshida, T.; Koga, N.; Morokuma, K. *Organometallics* **1996**, *15*, 766−777. (j) Margl, P.; Deng, L.; Ziegler, T. *Organometallics* **1998**, *17*, 933−946. (k) Deng, L.; Margl, P.; Ziegler, T. *J. Am. Chem. Soc.* **1997**, *119*, 1094−1100. (l) Lanza, G.; Fragala, I. L.; Marks, T. J. *Organometallics* **2001**, *20*, 4006−4017. (m) Lanza, G.; Fragala, I. L.; Marks, T. J. *Organometallics* **2002**, *21*, 5594−5612. (n) Novaro, O.; Blaisten- Barojas, E.; Clementi, E.; Giunchi, G.; Ruiz-Vizcaya, M. E. *J. Chem. Phys.* **1978**, *68*, 2337−2351. (o) Fujimoto, H.; Yamasaki, T.; Mizutani, H.; Koga, N. *J. Am. Chem. Soc.* **1985**, *107*, 6157−6161. (p) Kawamura- Kuribayashi, H.; Koga, N.; Morakuma, K. *J. Am. Chem. Soc.* **1992**, *114*, 2359−2366. (q) Koga, N.; Yoshida, T.; Morokuma, K. *Organometallics* **1993**, *12*, 2777−2787. (r) Weiss, H.; Ehrig, M.; Ahlrichs, R. *J. Am. Chem. Soc.* **1994**, *116*, 4919−4928. (s) Bierwagen, E. P.; Bercaw, J. E.; Goddard, W. A. *J. Am. Chem. Soc.* **1994**, *116*, 1481−1489. (t) Linnolahti, M.; Pakkanen, T. A. *Macromolecules* **2000**, *33*, 9205−9214. (u) Motta, A.; Fragala, I. L.; Marks, T. *J. Am. Chem. Soc.* **2008**, *130*, 16533−16546. (v) Yang, S. Y.; Ziegler, T. *Organometallics* **2006**, *25*, 887−900. (w) Guerra, G.; Corradini, P.; Cavallo, L. *Macromolecules* **2005**, *38*, 3973−3976. (x) Zhang, Y.; Ning, Y.; Caporaso, L.; Cavallo, L.; Chen, E. Y. X. *J. Am. Chem. Soc.* **2010**, *132*, 2695−2709.
(10) (a) Michalak, A.; Ziegler, T. *Organometallics* **1999**, *18*, 3998−4004. (b) Michalak, A.; Ziegler, T. *J. Am. Chem. Soc.* **2002**, *124*, 7519−7528. (c) Michalak, A.; Ziegler, T. *Kinet. Catal.* **2006**, *47*, 310−325. (d) Liu, Y.; Zhang, M.; Drew, M. G. B.; Yang, Z.; Liu, Y. *J. Mol. Struct.: THEOCHEM* **2005**, *726*, 277−283. (e) Yang, Z.; Liu, Y.; Liu, Y. *Chin. J. Struct. Chem.* **2005**, *24*, 723−728. (f) Liu, Y.; Liu, Y.; Drew, M. G. B. *Struct. Chem.* **2010**, *21*, 21−28. (g) Moscardi, G.; Resconi, L. *Organometallics* **2001**, *20*, 1918−1931. (h) Mitani, M.; Furuyama, R.; Mohri, J.; Saito, J.; Ishii, S.; Terao, H.; Nakano, T.; Tanaka, H.; Fujita, T. *J. Am. Chem. Soc.* **2003**, *125*, 4293−4305. (i) Borrelli, M.; Busico, V.; Cipullo, R.; Ronca, S. *Macromolecules* **2003**, *36*, 8171−8177. (j) Saßmannshausen, J. *Dalton Trans.* **2009**, 8993−8999. (k) Lee, J. W.; Jo, W. H. *J. Organomet. Chem.* **2009**, *694*, 3076−3083. (l) Caporaso, L.; Rosa, C. D.; Talarico, G. *J. Polym. Sci., Part A: Polym. Chem.* **2010**, *48*, 699−708.
(11) (a) Kirillov, E.; Lavanant, L.; Thomas, C.; Roisnel, T.; Chi, Y.; Carpentier, J. F. *Chem.—Eur. J.* **2007**, *13*, 923−935. (b) Landis, C. R.; Rosaaen, K. A.; Uddin, J. *J. Am. Chem. Soc.* **2002**, *124*, 12062−12063. (c) Zuccaccia, C.; Busico, V.; Cipullo, R.; Talarico, G.; Froese, R. D. J.; Vosejpka, P. C.; Hustad, P. D.; Macchioni, A. *Organometallics* **2009**, *28*, 5445−5458. (d) Manz, T. A.; Sharma, S.; Phomphrai, K.; Novstrup, K. A.; Fenwick, A. E.; Fanwick, P. E.; Medvedev, G. A.; Abu-Omar, M. M.; Delgass, W. N.; Thomson, K. T.; Caruthers, J. M. *Organometallics* **2008**, *27*, 5504−5520. (e) Manz, T. A.; Phomphrai, K.; Sharma, G. S.; Haq, J.; Novstrup, K. A.; Thomson, K. T.; Delgass, W. N.; Caruthers, J. M.; Abu-Omar, M. M. *J. Am. Chem. Soc.* **2007**, *129*, 3776−3777.
(12) (a) Tobisch, S.; Bögel, H.; Taube, R. *Organometallics* **1996**, *15*, 3563−3571. (b) Peluso, A.; Improta, R.; Zambelli, A. *Macromolecules* **1997**, *30*, 2219−2227. (c) Tobisch, S.; Bögel, H.; Taube, R. *Organometallics* **1998**, *17*, 1177−1196. (d) Tobisch, S.; Taube, R. *Organometallics* **1999**, *18*, 3045−3060. (e) Tobisch, S.; Taube, R. *Organometallics* **1999**, *18*, 5204−5218. (f) Peluso, A.; Improta, R.; Zambelli, A. *Organometallics* **2000**, *19*, 411−419. (g) Costabile, C.; Milano, G.; Cavallo, L.; Guerra, G. *Macromolecules* **2001**, *34*, 7952−7960. (h) Tobisch, S.; Taube, R. *Chem.—Eur. J.* **2001**, *7*, 3681−3695. (i) Tobisch, S. *Chem.—Eur. J.* **2002**, *8*, 4756−4766. (j) Tobisch, S.; Ziegler, T. *J. Am. Chem. Soc.* **2002**, *124*, 4881−4893. (k) Tobisch, S.; Ziegler, T. *J. Am. Chem. Soc.* **2002**, *124*, 13290−13301. (l) Tobisch, S. *Macromolecules* **2003**, *36*, 6235−6244. (m) Tobisch, S.; Taube, R. *J. Organomet. Chem.* **2003**, *683*, 181−190. (n) Tobisch, S. *Chem.—Eur. J.* **2003**, *9*, 1217−1232. (o) Tobisch, S. *J. Am. Chem. Soc.* **2003**, *126*, 259−272. (p) Tobisch, S. *Organometallics* **2003**, *22*, 2729−2740. (q) Tobisch, S. *Macromolecules* **2003**, *36*, 6235−6244. (r) Tobisch, S.; Werner, H. *Dalton Trans.* **2004**, 2963−2968. (s) Tobisch, S. *Can. J. Chem.* **2009**, *87*, 1392−1405. (t) Tobisch, S. *J. Am. Chem. Soc.* **2004**, *126*, 259−272. (u) Costabile, C.; Capacchione, C.; Saviello, D.; Proto, A. *Macromolecules* **2012**, *45*, 6363−6370. (v) Costabile, C.; Milano, G.; Cavallo, L.; Longo, P.; Guerra, G.; Zambelli, A. *Polymer* **2004**, 467−485.
(13) (a) Perrin, L.; Bonnet, F.; Visseaux, M.; Maron, L. *Chem. Commun.* **2010**, *46*, 2965−2967. (b) Perrin, L.; Bonnet, F.; Chenal, T.; Visseaux, M.; Maron, L. *Chem.—Eur. J.* **2010**, *16*, 11376−11385. (c) Li, X.; Nishiura, M.; Hu, L.; Mori, K.; Hou, Z. *J. Am. Chem. Soc.* **2009**, *131*, 13870−13882. (d) Zhang, L.; Suzuki, T.; Luo, Y.; Nishiura, M.; Hou, Z. *Angew. Chem., Int. Ed.* **2007**, *46*, 1909−1913. (e) Li, X.; Nishiura, M.; Hu, L.; Mori, K.; Hou, Z. *J. Am. Chem. Soc.* **2009**, *131*, 13870−13882. (f) Zhang, L.; Luo, Y.; Hou, Z. *J. Am. Chem. Soc.* **2005**, *127*, 14562−14563. (g) Luo, Y.; Hou, Z. *Organometallics* **2006**, *25*, 6162−6165. (h) Kang, X.; Song, Y.; Luo, Y.; Li, G.; Hou, Z.; Qu, J. *Macromolecules* **2012**, *45*, 640−651.
(14) Taube, R.; Gehrke, J.; Radeglia, R. *J. Organomet. Chem.* **1985**, *291*, 101−115.
(15) *Gaussian 09, Revision A.02*: Frisch, M. J.; Trucks, G. W.; Schlegel, H. B.; Scuseria, G. E.; Robb, M. A.; Cheeseman, J. R.; Scalmani, G.; Barone, V.; Mennucci, B.; Petersson, G. A.; Nakatsuji, H.; Caricato, M.; Li, X.; Hratchian, H. P.; Izmaylov, A. F.; Bloino, J.; Zheng, G.; Sonnenberg, J. L.; Hada, M.; Ehara, M.; Toyota, K.; Fukuda, R.; Hasegawa, J.; Ishida, M.; Nakajima, T.; Honda, Y.; Kitao, O.; Nakai, H.; Vreven, T.; Montgomery, Jr., J. A.; Peralta, J. E.; Ogliaro, F.; Bearpark, M.; Heyd, J. J.; Brothers, E.; Kudin, K. N.; Staroverov, V. N.; Kobayashi, R.; Normand, J.; Raghavachari, K.; Rendell, A.; Burant, J. C.; Iyengar, S. S.; Tomasi, J.; Cossi, M.; Rega, N.; Millam, N. J.; Klene, M.; Knox, J. E.; Cross, J. B.; Bakken, V.; Adamo, C.; Jaramillo, J.; Gomperts, R.; Stratmann, R. E.; Yazyev, O.; Austin, A. J.; Cammi, R.; Pomelli, C.; Ochterski, J. W.; Martin, R. L.; Morokuma, K.; Zakrzewski, V. G.; Voth, G. A.; Salvador, P.; Dannenberg, J. J.; Dapprich, S.; Daniels, A. D.; Farkas, Ö.; Foresman, J. B.; Ortiz, J. V.; Cioslowski, J.; Fox, D. J. Gaussian, Inc., Wallingford, CT, 2009.
(16) (a) Beck, A. D. *J. Chem. Phys.* **1993**, *98*, 5648−5652. (b) Lee, C. T.; Yang, W. T.; Parr, R. G. *Phys. Rev. B* **1988**, *37*, 785−789. (c) Perdew, J. P.; Burke, K.; Wang, Y. *Phys. Rev. B* **1996**, *54*, 16533−16539.
(17) (a) Dolg, M.; Wedig, U.; Stoll, H.; Preuss, H. *J. Chem. Phys.* **1987**, *86*, 866−872. (b) Schwerdtfeger, P.; Dolg, M.; Schwarz, W. H. E.; Bowmaker, G. A.; Boyd, P. D. W. *J. Chem. Phys.* **1989**, *91*, 1762−1774. (c) Dolg, M.; Stoll, H.; Savin, A.; Preuss, H. *Theor. Chim. Acta* **1989**, *75*, 173−194. (d) Andrae, D.; Haeussermann, U.; Dolg, M.; Stoll, H.; Preuss, H. *Theor. Chim. Acta* **1990**, *77*, 123−141. (e) Dolg, M.; Stoll, H.; Preuss, H. *Theor. Chim. Acta* **1993**, *85*, 441−450. (f) Bergner, A.; Dolg, M.; Kuechle, W.; Stoll, H.; Preuss, H. *Mol. Phys.* **1993**, *80*, 1431−1441.
(18) Höllwarth, A.; Böhme, M.; Dapprich, S.; Ehlers, A. W.; Gobbi, A.; Jonas, V.; Höhler, K. F.; Stegmann, R.; Veldkamp, P.; Frenking, G. *Chem. Phys. Lett.* **1993**, *208*, 237−240.

(19) Marenich, A. V.; Cramer, C. J.; Truhlar, D. G. *J. Phys. Chem. B* **2009**, *113*, 6378−6396.
(20) (a) Kretschmer, W. P.; Meetsma, A.; Hessen, B.; Schmalz, T.; Qayyum, S.; Kempe, R. *Chem.—Eur. J.* **2006**, *12*, 8969−8978. (b) Boisson, C.; Monteil, V.; Ribour, D.; Spitz, R.; Barbotin, F. *Macromol. Chem. Phys.* **2003**, *204*, 1747−1754.
(21) The M06 functional showed good performance in the studies of organometallic reactions and binding energies; see: Zhao, Y.; Truhlar, D. G. *Theor. Chem. Acc.* **2008**, *120*, 215−241. For D3 dispersion correction, see: Grimme, S.; Antony, J.; Ehrlich, S.; Krieg, H. *J. Chem. Phys.* **2010**, *132*, 154104.
(22) Lynch, B. J.; Truhlar, D. G. *J. Phys. Chem. A* **2003**, *107*, 3898−3906.
(23) Ionic Radii in Crystals. In *CRC Handbook of Chemistry and Physics*, 90th ed. (CD-ROM version); Lide, D. R., Ed.; CRC Press/Taylor and Francis: Boca Raton, FL, 2010.